RMetS

Royal Meteorological Society

Short Communication

Local atmospheric decoupling in complex topography alters climate change impacts

Christopher Daly,* David R. Conklin and Michael H. Unsworth

Department of Geosciences, 2000 Kelley Engineering Center, Oregon State University, Corvallis, OR 97331, USA

ABSTRACT: Cold air drainage and pooling occur in many mountain valleys, especially at night and during winter. Local climate regimes associated with frequent cold air pooling have substantial impacts on species phenology, distribution and diversity. However, little is known about how the degree and frequency of cold air drainage and pooling will respond to a changing climate. Evidence suggests that, because cold pools are decoupled from the free atmosphere, these local climates may not respond in the same way as regional-scale climates estimated from coarse-grid general circulation models. Indeed, recent studies have demonstrated that historical changes in the frequency of synoptic conditions have produced complex spatial variations in the resulting climatic changes on the ground. In the mountainous terrain of the Oregon Cascades, we show that, at relatively exposed hill slope and ridge top locations, air temperatures are highly coupled to changes in synoptic circulation patterns at the 700-hPa level, whereas in sheltered valley bottoms, cold air pooling at night and during winter causes temperatures to be largely decoupled from, and relatively insensitive to, 700-hPa flow variations. The result is a complex temperature landscape composed of steep gradients in temporal variation, controlled largely by gradients in elevation and topographic position. When a projected climate warming of 2.5 °C was combined with likely changes in the frequency distribution of synoptic circulation, modelled temperature changes at closely spaced locations diverged widely (by up to 6 °C), with differences equalling or exceeding that of the imposed regional temperature change. Because cold air pooling and consequent atmospheric decoupling occur in many mountain valleys, especially at high latitudes, this phenomenon is likely to be an important consideration in understanding the impacts of climate change in mountainous regions. Copyright © 2009 Royal Meteorological Society

Supporting information may be found in the online version of this article.

1. Introduction

Cold air drainage and pooling in mountain valleys have been recognised and studied for more than a century (e.g. Marvin, 1914 and Ekhart, 1934; see reviews by Geiger, 1966; Whiteman, 2000; Barry, 2008; Poulos and Zhong, 2008). The development of this thermally driven phenomenon depends on synoptic meteorological conditions, and it is well-developed during periods of low solar radiation, high atmospheric pressure and light synoptic winds (Barr and Orgill, 1989; Beniston, 2006; Lundquist and Cayan, 2007). In such conditions, when the radiation balance becomes negative, such as near sunset on a clear day, long wave radiation losses become larger than short wave radiation gains, and the surface cools. As air near the ground is subsequently cooled,

it forms a shallow stable layer (Whiteman, 2000). In a valley or on a slope, this surface layer is cooler and denser than free air at the same elevation. Consequently, the dense air drains downslope and is replaced by warmer air from aloft, which is subsequently cooled, continuing the cycle. Cold air will pool and stagnate in local depressions and valley constrictions (Gustavsson *et al.*, 1998; Lindkvist *et al.*, 2000; Lundquist *et al.*, 2008), forming temperature inversions that can range from a few to hundreds of metres in depth, depending on valley geometry, duration of the negative energy balance and synoptic conditions (McKee and O'Neal, 1989; Whiteman, 2000; Clements *et al.*, 2003). The lack of vertical mixing within these valley temperature inversions effectively decouples air within the inversion from the free atmosphere above (Whiteman, 2000).

There is ample evidence that cold air pooling and resulting atmospheric decoupling are widespread (Miller *et al.*, 1983; McChesney *et al.*, 1995; Gustavsson *et al.*,

* Correspondence to: Christopher Daly, Department of Geosciences, 2000 Kelley Engineering Center, Oregon State University, Corvallis, OR 97331, USA. E-mail: chris.daly@oregonstate.edu

1998; Lindkvist *et al.*, 2000; Clements *et al.*, 2003; Zangl, 2005; Chung *et al.*, 2006; Lundquist *et al.*, 2008), even to some degree in the subtropics (Daly *et al.*, 2003) and in very gentle terrain (Mahrt *et al.*, 2001). Local climate regimes associated with frequent cold air pooling have substantial impacts on species phenology, distribution and diversity (Tenow and Nilssen, 1990; McChesney *et al.*, 1995; Blennow and Lindkvist, 2000; Rodrigo, 2000; Chung *et al.*, 2006). However, little is known about how the degree and frequency of cold air pooling will respond to a changing climate. General circulation models (GCMs) used to simulate future climate changes are too coarse-grained (50 km or greater) to simulate cold air pooling and other fine-scale topographically defined climates (e.g. PCMDI archive http://www-pcmdi.llnl.gov/ipcc/about_ipcc.php). Most climate change projections derived from GCM simulations (e.g. by downscaling) therefore carry a high degree of regional coherence, where simulated local climate change is closely coupled to simulated regional change (Beaumont *et al.*, 2007; Ashcroft *et al.*, 2009). Because cold pools are decoupled from the free atmosphere, they may, in reality, respond differently than the regional pattern (Lundquist *et al.*, 2008). For example, failure to account for topographic position (e.g. valley *vs* ridge) is a possible reason why there has been conflicting evidence as to whether climate is changing more rapidly at higher elevations than at lower elevations (Pepin and Norris, 2005; Beniston, 2006; Pepin and Lundquist, 2008). Recently, it has been demonstrated that historical changes in the frequency of synoptic conditions have produced complex spatial variations in the resulting climatic changes on the ground (Lundquist and Cayan, 2007; Ashcroft *et al.*, 2009). This study seeks to further investigate the degree of local-to-regional climate decoupling in a mountainous location, and attempts to quantify the implications for future climate projections.

2. Study area

We investigated the concept of local-to-regional climate decoupling using a unique set of long-term temperature observations at the HJ Andrews Experimental Forest (HJA), a mountainous Long Term Ecological Research site on the western slope of the Cascade Mountains in Oregon, USA (Andrews, 2007; Figure 1). Elevations of the 6400-ha HJA range from 412 m in the lowest drainages in the west to 1627 m on the highest ridgelines in the east. The HJA is generally representative of the rugged mountainous landscape of the Pacific Northwest, and is heavily vegetated with conifer-dominated forests.

The climate of the HJA is Mediterranean, characterised by wet winters and dry summers; approximately 75% of the annual precipitation falls during the months of November–April. During winter, the polar jet stream brings a series of moist frontal systems from the Pacific Ocean onshore into the region. Located on the western or windward slopes of the Cascade Range, the HJA receives orographically enhanced precipitation that typically increases with elevation. Observed annual precipitation for the period 1971–2000 ranges from 2227 mm/year at 430 m to 2712 mm/year at 1294 m. Temperatures are typically mild throughout the year, owing to the moderating influence of marine air from the Pacific Ocean. The Cascade Crest usually serves as an effective barrier to cold air outbreaks originating in interior Canada. Snow is relatively rare below 500 m,
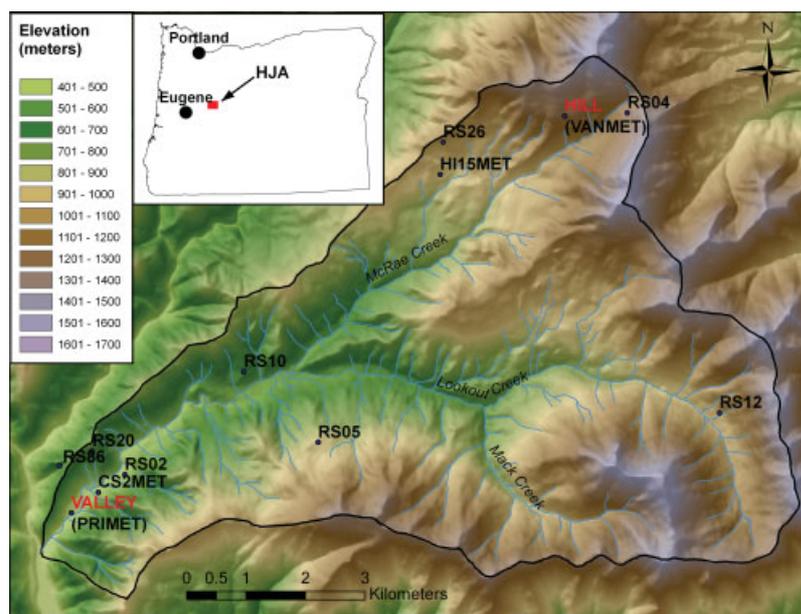
Figure 1. Topographic relief map with locator insert for the HJ Andrews Experimental Forest (HJA). Locations of stations used in the analysis, including VALLEY (PRIMET) and HILL (VANMET), are shown. This figure is available in colour online at www.interscience.wiley.com/ijoc

but a substantial seasonal snowpack accumulates above 900 m. Mean 1971–2000 January minimum temperatures at 430 m and 1294 m are −1.3 and −2.5 °C, respectively, and July maximum temperatures are 28.6 and 22.1 °C, respectively.

The steep, deeply incised slopes and narrow valleys are highly susceptible to cold air drainage and pooling (Daly *et al*., 2007; Pypker *et al*., 2007). In situations with a negative radiation balance and low wind speeds, temperatures stratify quickly with cool, dense air draining into local valleys and depressions. As a result, temperature inversions are established; temperature increases rather than decreases with height in a layer near the ground, sharply transitioning to the more typical temperature decrease with height above this layer (Daly *et al*., 2007).

3. Example of temperature decoupling

Temperatures at two HJA stations (available at http://www.fsl.orst.edu/lter/) provide a striking example of temporal decoupling. PRIMET station, hereafter called 'VALLEY,' is located in a valley bottom at 430 m elevation (Table I). VANMET station, hereafter called 'HILL,' is located 10 km to the northeast, high on a south-facing hill slope at 1273 m. Time series of vertical temperature gradients in daily maximum (T_{max}) and minimum (T_{min}) temperatures (i.e. ΔT_{HVmax} and ΔT_{HVmin}, the differences between the daily temperatures at HILL and VALLEY, divided by their elevation difference in km) were constructed for the period 1987–2005. If temperature variations were synchronous and of equal magnitude between the sites, the vertical temperature gradient would, by definition, be invariant. This was clearly not the case for these two stations (plotted only for the years 1995–1999 for clarity in Figure 2). ΔT_{HVmax} was relatively constant during spring and summer, and approximated the mean environmental lapse rate in the troposphere of about −6.5 °C/km. However, variability increased dramatically in fall and
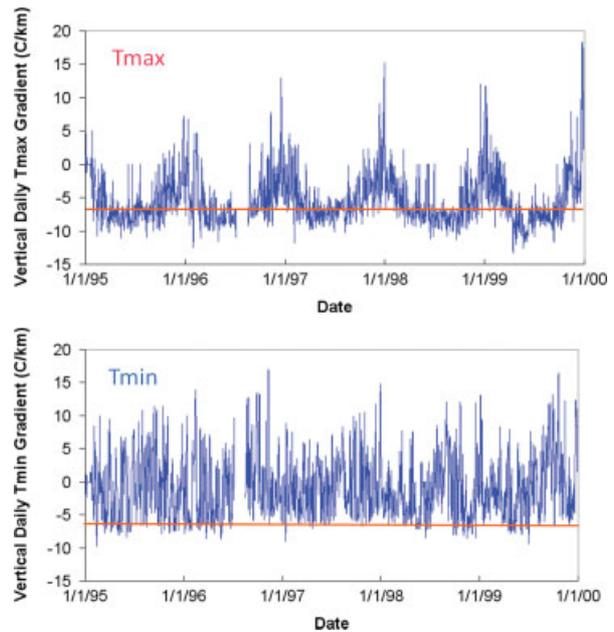
Figure 2. Time series plots of ΔT_{HVmax} and ΔT_{HVmin} (Hill–Valley daily T_{max} and T_{min} differences, respectively, expressed in °C/km elevation), for the period January 1995–December 1999. Orange horizontal line represents a constant, fully synchronous, vertical daily temperature gradient at the environmental (global mean) lapse rate of −6.5 °C/km. T_{max} and T_{min} are clearly asynchronous between these two sites, and ΔT_{HVmax} and ΔT_{HVmin} are often much less negative than the environmental lapse rate. ΔT_{HVmax} shows a clear seasonal cycle in vertical gradient, while ΔT_{HVmin} does not. This figure is available in colour online at www.interscience.wiley.com/ijoc

winter. Although HILL is more than 800 m higher in elevation than VALLEY, it was sometimes as much as 15 °C warmer than VALLEY. Such temperature inversions are the result of cold air pooling in the valley, but not on the hill slope. For T_{min}, the day-to-day vertical gradient was highly variable during all seasons. Inversions dominated ΔT_{HVmin} much of the time, confirming that nocturnal cold air pooling can and does occur year round in this region (Daly *et al*., 2007; Pypker *et al*., 2007).

Table I. HJA meteorological stations used in the analysis.

Meteorological station	Location (Easting, Northing, UTM Zone 10)	Elevation (m)	Topographic index (m)
VALLEY (PRIMET)	559563, 4895461	430	1
HILL (VANMET)	567832, 4902239	1273	23
CS2MET	560044, 4895780	460	8
HI15	565859, 4901219	922	10
RS02	560513, 4896132	490	15
RS04	568985, 4902368	1310	28
RS05	563769, 4896670	880	14
RS10	562474, 4897908	610	19
RS12	570409, 4897130	1007	14
RS20	559997, 4896597	683	30
RS26	565992, 4901852	1040	24
RS86	559377, 4896330	653	29

4. Dependence of Temperature Decoupling on Atmospheric Circulation Patterns

We investigated the dependence of this spatial decoupling of temperature on atmospheric circulation using an analysis (Losleben *et al.*, 2000) based on the NCEP/NCAR reanalysis data set (Kalnay *et al.*, 1996). Daily circulation indices (see Supporting Information) were calculated for the period 1987–2005 from a sub-grid of the reanalysis pressure height data set for the 700-hPa ($\sim$3000 m) level, centered over northwestern Oregon (Figure S1, Supporting Information). We found that the mean daily ΔT_{HVmin} was closely related to a combination of flow strength and vorticity (curvature) of airflow in the troposphere (Figure 3). The combination of anti-cyclonic flow curvature and low flow strength produced the strongest T_{min} inversions, with a year round mean ΔT_{HVmin} of about $+3.5\,^{\circ}$C/km. Such conditions – light winds, strong nocturnal cooling under clear skies, and little vertical mixing under high pressure – allow the development of cold air drainage and pooling in sheltered valleys. In contrast, a cyclonic pattern with high flow strength, giving well-mixed, well-ventilated conditions, had the most negative mean ΔT_{HVmin} of about $-4\,^{\circ}$C/km. This is consistent with previous studies of nocturnal valley drainage winds (e.g. Barr and Orgill, 1989).

Does spatial decoupling, and its relationship to upper-level flow patterns, persist to the monthly time interval? The monthly time step is important in many natural resource models and analyses, especially those used for multi-annual simulations (e.g., MC1, Daly *et al.*, 2000; PnET, Aber *et al.*, 2005; and 2PG, Landsberg and Waring, 1997). A simplified upper-level flow index that relies on flow curvature alone was developed to summarise each month's weather patterns in the NCEP reanalysis.
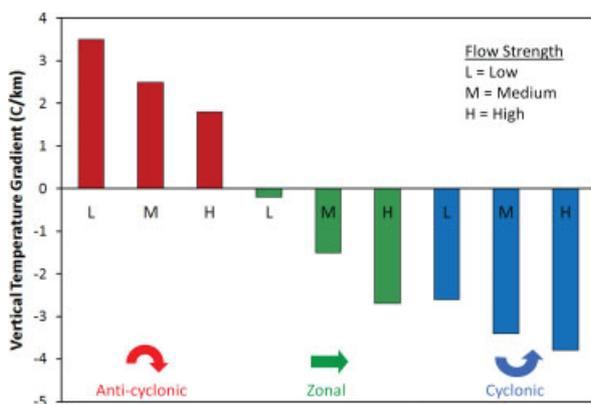
Figure 3. Relationship between 700-hPa ($\sim$3000 m) flow strength and curvature and mean daily ΔT_{HVmin} for all days in the period 1987–2005. Cyclonic, or troughing, curvature days are often cloudy and wet with good atmospheric mixing. Anti-cyclonic or ridging, curvature days are generally clear and dry with poor atmospheric mixing. Zonal flow, with little curvature, exhibits weather that is transitional between cyclonic and anti-cyclonic conditions. Each flow curvature pattern was divided into three flow strength categories: low, medium and high. Average ΔT_{HVmin} follows a smooth transition from positive in the low flow strength anti-cyclonic flow category to negative in the high flow strength cyclonic flow category. This figure is available in colour online at www.interscience.wiley.com/ijoc

This index, hereafter referred to as A–C, was defined as the number of anti-cyclonic days minus the number of cyclonic days in the month. A–C can therefore range from -31 to $+31$, and is zero if there are an equal number of days with cyclonic and anti-cyclonic flow (zonal days, those with little flow curvature, are not counted).

Linear regression functions between the monthly A–C index, and the monthly means of daily T_{min} and T_{max} were developed for May and December at HILL and VALLEY for the years 1987–2005 (Figure 4). These two months provide a strong contrast. May is a month when solar elevation is high, and daytime atmospheric mixing and ventilation are generally good. In December, low solar elevations and long nights allow for extended and frequent periods of radiational cooling, which can lead to persistent cold air drainage and temperature inversions when synoptic winds are light.

Temperature data were relatively complete for these months; VALLEY had data for 17 out of 19 Mays and 18 out of 19 Decembers during the 1987–2005 period, and HILL had complete data for both months. A month was considered 'complete' if it had at least 75% of days with valid data. To create a continuous data set at VALLEY, temperature data from CS2MET, a nearby station with very similar elevation and topographic position (Table I; Figure 1), were used for the months of December 1994 and May 2000.

Slopes and intercepts from these linear regression functions between the monthly A–C index and the monthly means of daily T_{min} and T_{max} (Figure 4) were in turn used to produce the estimated T_{min} and T_{max} traces in Figure 5. In both May and December, observed HILL T_{max} and T_{min} were explained well by the A–C index (Figures 4 and 5), T_{max} more so than T_{min}. However, temperatures at VALLEY were responsive to the A–C index only for May T_{max}, when the atmosphere was well-mixed. Thus, even at the monthly scale, the differing responsiveness between sites of local temperature to synoptic air flow produced temporally varying differences in the monthly mean T_{max} and T_{min} between HILL and VALLEY.

5. Implications for Climate Change

How would spatial decoupling modify the local temperature response to global warming? We conducted sensitivity tests to assess the effects of downscaling regional climate change projections to HJA. Under the moderate A1B emissions scenario of the IPCC, temperatures in western Oregon are projected to warm $2–3\,^{\circ}$C by the year 2100 (IPCC, 2007). Although general circulation modelling has not focused on flow pattern analysis, most models predict that the polar jet stream and subtropical high-pressure belt will shift northwards, suggesting that western Oregon would experience a more pronounced Mediterranean climate with extended summer drought, and fewer days with precipitation during winter (IPCC, 2007). Given that anti-cyclonic days are generally dry with high surface pressure, and cyclonic days are often
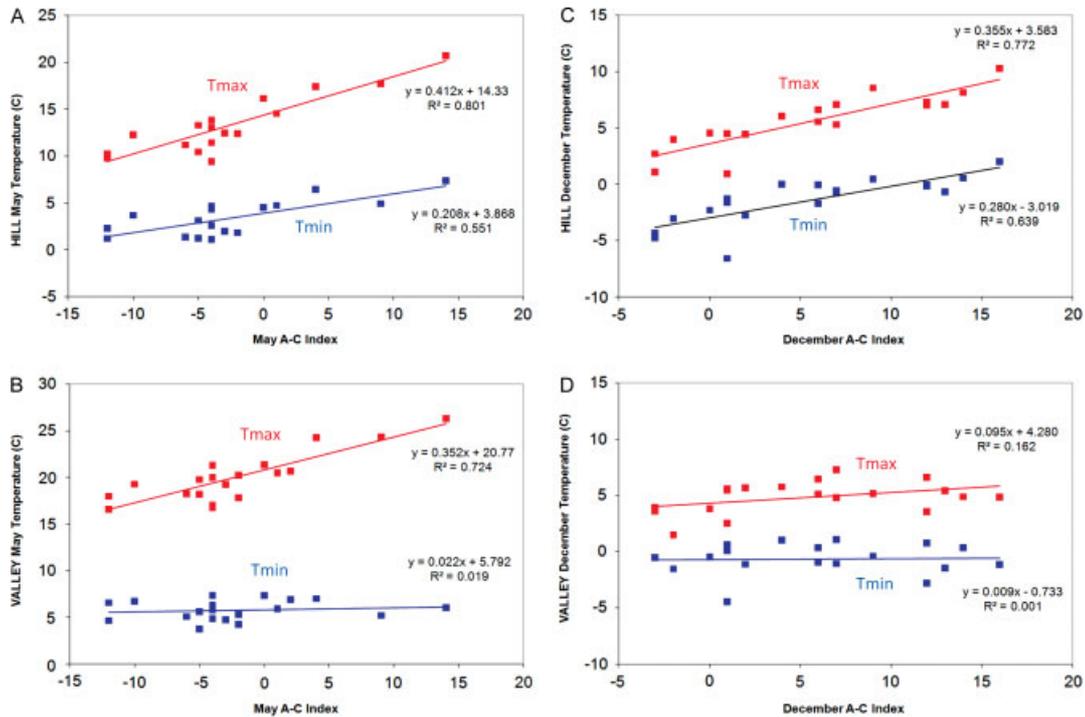
Figure 4. Scatter plots and regression functions between the A–C index and T_{min} and T_{max} at HILL and VALLEY for the months of May (A, B) and December (C, D). These regression functions were used to make the temperature estimates shown in Figure 5. This figure is available in colour online at www.interscience.wiley.com/ijoc

wet with low surface pressure, the model projections are consistent with an increase in the relative number of anti-cyclonic or effectively similar days in winter. This, in turn, translates into an increase in the monthly A–C index. As a sensitivity test, temperature projections for December T_{max} at VALLEY and HILL were made for the year 2100, assuming a regional 2.5 °C temperature increase, accompanied by an increase in the A–C index. At HILL, each increase of one day in the A–C index was associated with an increase in the December average daily T_{max} of 0.36 °C, while at VALLEY the corresponding increase was only 0.10 °C. (Given the limited ability of the A–C index to predict December average daily T_{max} at VALLEY, an argument could be made that the increase is essentially zero.) An increase of 10 days in the A–C index (about one third of the historical range of December A–C in this region) would thus raise the difference between December T_{max} at HILL and December T_{max} at VALLEY (ΔT_{HVmax}) by 2.6 °C, an amount larger than the projected 2.5 °C regional warming itself.

Differential responses of T_{max} and T_{min} at HILL and VALLEY, given increases in the A–C index of 5 and 10 days, are shown for all months in Figure 6. T_{max} differences were largest in winter, when cold air pooling occurs both day and night at VALLEY, but not at HILL. T_{min} differences were relatively consistent from month to month, because nocturnal cold air pooling was present throughout the year at VALLEY, but not at HILL. Differences tended to be largest in the fall, when clear, calm conditions and relatively low sun angles allowed cold air pooling to occur frequently and for longer periods. August temperatures were not responsive

to changes in the A–C index at either station, apparently because August temperatures exhibited relatively little variation from year to year.

Are these projections of spatial temperature decoupling spatially robust? Mean December T_{max} data were available from a total of 12 temperature stations within the HJA which had at least 12 years of data during the period 1987–2005 (VALLEY, HILL and 10 others, Table I). As was done for HILL and VALLEY, slopes of the regression function relating December T_{max} to the A–C index were calculated for the additional 10 stations. To create a spatial representation, this slope was entered as the dependent variable into a multiple regression function with elevation and topographic index as independent variables. Topographic index describes the vertical position of a site relative to the surrounding terrain; sheltered valley-bottom sites have low topographic indexes, whereas exposed ridge-top sites have high indexes (Daly *et al.*, 2008; Figure S2, Supporting Information). Elevation estimates were obtained from a 50-m resolution digital elevation model (DEM). A series of calculations using the 50-m DEM determined that a highly localised topographic index, calculated within a diameter of 150 m, explained the most variance (63%) in the slope of the December T_{max} *vs* A–C regression function. When the 150-m topographic index was combined with elevation in multiple linear regression, the resulting model

$$Slope = 0.003303 + 0.000124 \, (elevation)$$
$$+ 0.005934 \, (topoindex)$$
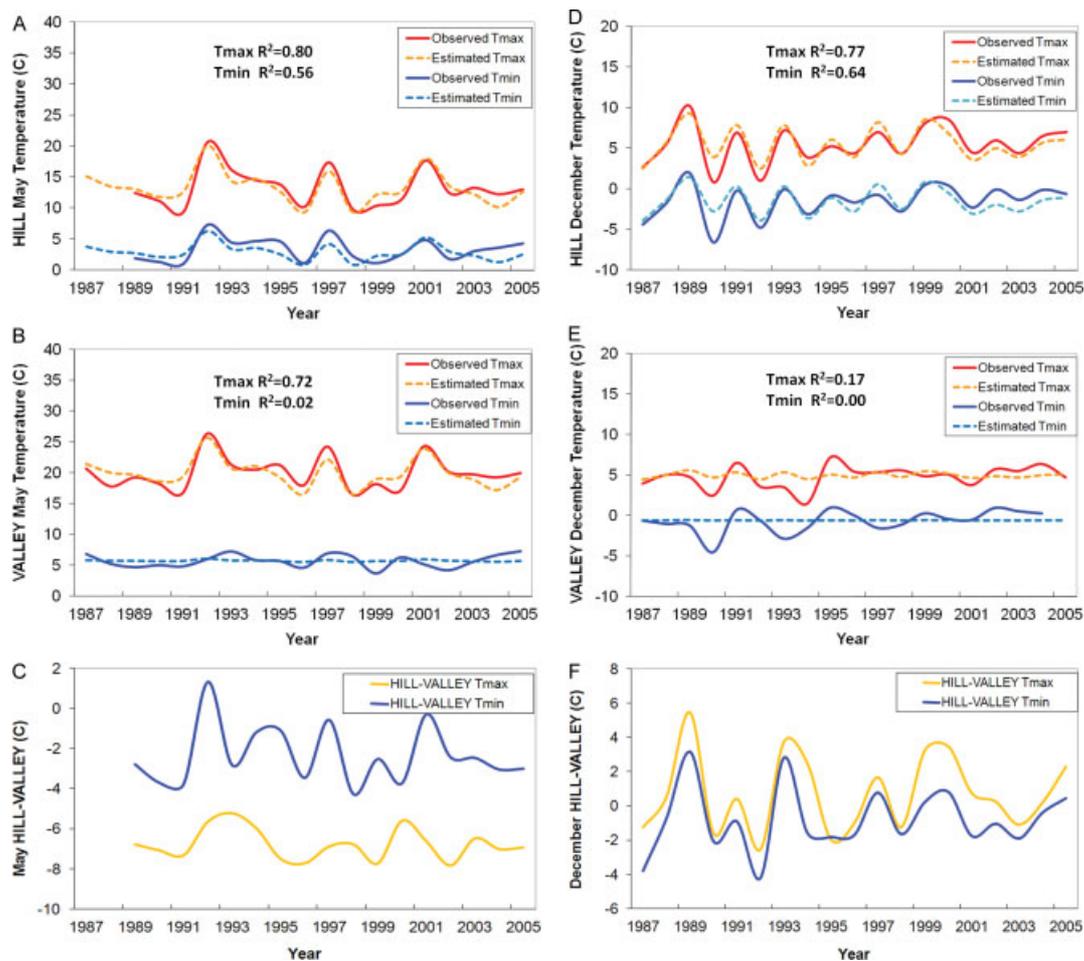
Figure 5. Observed and estimated HILL and VALLEY monthly mean T_{max} and T_{min}, and ΔT_{HVmax} and ΔT_{HVmin} (HILL−VALLEY temperature differences, expressed in°C/km), for the months of May (A,B,C) and December (D,E,F). Temperatures were estimated through linear regression with the A–C index, the difference in frequency of anti-cyclonic and cyclonic days in a month. In both May and December, HILL T_{max} and T_{min} were very responsive to, and accurately estimated by, the A–C index. However, VALLEY was responsive only for May T_{max}, when the atmosphere was well-mixed. At night in May, and during both day and night in December, cold air pooling left VALLEY temperature variations relatively damped and unresponsive to upper-air fluctuations. As a result, HILL and VALLEY temperature variations were rarely synchronised, even at the monthly time step. (Temperatures were plotted with the Excel smooth line option to improve readability). This figure is available in colour online at www.interscience.wiley.com/ijoc

explained 82% of the variance in the slope of the relationship between December T_{max} and A–C index. The elevation and topographic index predictors were not completely independent, but the relationship between the two was not strong ($R^2 = 0.21$). As might be expected, stations on locally elevated terrain were somewhat more likely to be located at high elevations than stations in local depressions. For comparison, the same multiple regression was also run for May T_{min}. The combined elevation–topographic index explained 84% of the variance in the slope of the May T_{min} *vs* A–C index, but in this case topographic index explained only 47% of the variance.

We used our simple model of the spatial distribution of atmospheric coupling to map projected T_{max} changes for December 2100 across the HJA, assuming a 10-day increase in the A–C index, and a 2.5 °C regional warming over the century (Figure 7). In Figure 7, the change in T_{max} due to the change in atmospheric coupling is added to the 2.5 °C regional warming. Mapped T_{max} changes

range from less than 3 °C in low-elevation valleys to more than 8 °C on the high-elevation ridge-tops. Intricate patterns of elevation and topographic position create steep response gradients across the landscape. For example, there is a greater than 2 °C difference in projected December T_{max} increase between VALLEY and station RS86, which is on a ridge 200 m higher and less than 1 km away (Figure 7). Moreover, it is likely that the true gradients and patterns may be even steeper and more complex than what our simple model suggests. Other potentially important factors not accounted for include slope and aspect, proximity to streams, snow cover, horizon shading by terrain and forest canopy coverage.

6. Conclusions

This study suggests that for mountainous regions, local variation in temperature increase is likely to be less spatially coherent than the temperature increase predicted
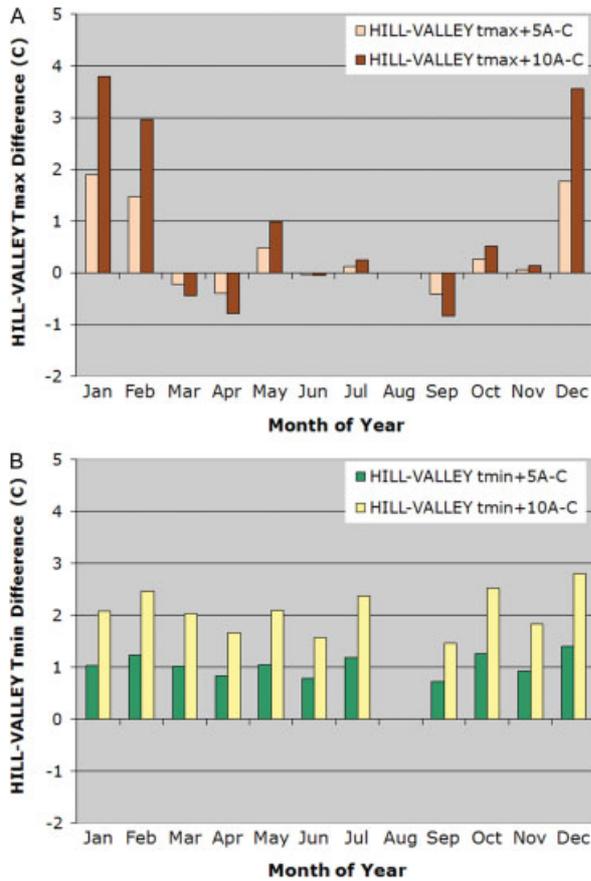
Figure 6. Differences in (a) T_{max} and (b) T_{min} responses between HILL and VALLEY for each month, given increases in the A–C index of 5 and 10 days. T_{max} differences are largest in winter, when cold air pooling can occur at both day and night due to low sun angles. T_{min} differences are relatively constant throughout the year, but tend to be largest in the fall, when clear, calm conditions are more common. This figure is available in colour online at www.interscience.wiley.com/ijoc

by global and regional models. This has implications for impacts on ecosystems and biodiversity. While locations subject to frequent cold air pooling are not likely to escape regionally increasing temperatures, our analysis in Oregon suggests that they may act as refugia (Pearson, 2006) against the amplified temperature trends and variations that we predict will occur on adjacent hill slopes and crests if anti-cyclonic conditions become more frequent (e.g. Figure 5, compare panels D and E). Other areas located in the transition zone between the mid-latitude westerlies and the subtropical high-pressure belt (i.e. those with a Mediterranean climate such as southern Europe, southern Africa, and mid-latitude South America), may also see an increase in the frequency of anti-cyclonic conditions and similar discrepancies in local temperature changes. The picture is likely to be different in regions for which the frequency of anti-cyclonic days is expected to decrease, rather than increase. In these areas, the strength and frequency of cold air pooling events would diminish. Given that the mean lapse rate is steeper during cyclonic conditions than anti-cyclonic conditions (Figure 3), local differences in temperature increases between depressions and adjacent hill slopes and crests would likely be muted or even reversed, with hill slopes and crests experiencing less warming than depressions.

Clearly not all mountainous regions are like the HJ Andrews, with its steep ridges and poorly ventilated valleys, prime topographic conditions for the development of persistent cold air pools and inversions. However, such topography is widespread in the Oregon and Washington Cascades, and also occurs in the Sierra Nevada, Rocky Mountains and other mountain chains worldwide. In addition, highly localised topographic position appears to be important in determining the response of a site to synoptic variations at HJA, suggesting that cold air pooling that occurs in small depressions in many regions
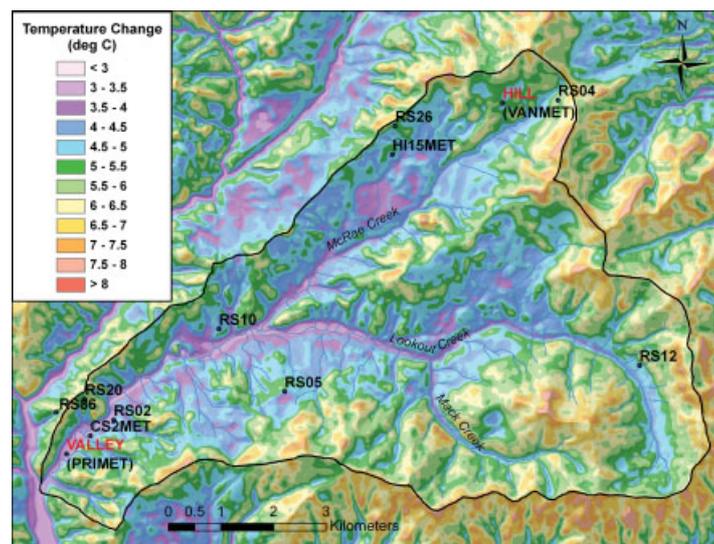
Figure 7. Estimated spatial distribution of December T_{max} response to a 2.5 °C regional temperature increase and a 10-day increase in the A–C index across the HJA (outlined in black). T_{max} response was modeled with multiple regression for 12 stations (shown on map) using elevation and local topographic position as explanatory variables. Intricate patterns of elevation and topographic position create steep response gradients across the landscape. This figure is available in colour online at www.interscience.wiley.com/ijoc

is climatically significant. Further research is warranted to determine the geographic applicability of the conditions described in this study.

Much work has already been done to demonstrate the dependence of temperature decoupling on synoptic flow characteristics. If further investigations confirm that the degree of spatial decoupling in regions of interest (e.g. mid-latitudes) can be estimated from indices similar to the simple anti-cyclonic–cyclonic (A–C) frequency at a monthly time interval, an important step for climate modelers will be to test the ability of their models to reproduce past synoptic flow pattern frequency. Together with continued development of statistical and dynamical downscaling techniques, simulating such patterns faithfully should greatly improve our ability to predict future local climate impacts in mountainous terrain.

Acknowledgements

References

Aber JD, Ollinger SV, Driscoll CT, Federer CA, Reich PB. 2005. *Photosynthetic/Evapo-Transpiration model (PnET)*. Model product available on-line at http://daac.ornl.gov [accessed: 2009].

Ashcroft MB, Chisholm LA, French KO. 2009. Climate change at the landscape scale: predicting fine-grained spatial heterogeneity in warming and potential refugia for vegetation. *Global Change Biology* **15**: 656–667.

Barr S, Orgill MM. 1989. Influence of external meteorology on nocturnal valley drainage winds. *Journal of Applied Meteorology* **28**: 497–517.

Barry RG. 2008. *Mountain Weather and Climate*. Cambridge University Press: Cambridge, 506 pp.

Beaumont LJ, Pitman AJ, Poulsen M, Hughes L. 2007. Where will species go? Incorporating new advances in climate modelling into projections of species distributions. *Global Change Biology* **13**: 1368–1385.

Beniston M. 2006. Mountain weather and climate: a general overview and a focus on climate change in the Alps. *Hydrobiologia* **562**: 3–16.

Blennow K, Lindkvist L. 2000. Models of low temperature and high irradiance and their application to explaining the risk of seedling mortality. *Forest Ecology and Management* **135**: 289–301.

Clements CB, Whiteman CD, Horel JD. 2003. Cold-air-pool structure and evolution in a mountain basin: Peter Sinks, Utah. *Journal of Applied Meteorology* **42**: 752–768.

Chung U, Seo HH, Hwang KH, Hwang BS, Choi JJ, Lee T, Yun JI. 2006. Minimum temperature mapping over complex terrain by estimating cold air accumulation potential. *Agricultural and Forest Meteorology* **137**: 15–24.

Daly C, Bachelet D, Lenihan JM, Neilson RP, Parton WJ, Ojima D. 2000. Dynamic simulation of tree-grass interactions for global change studies. *Ecological Applications* **10**: 449–469.

Daly C, Halbleib MD, Smith JI, Gibson WP, Doggett MK, Taylor GH, Curtis J, Pasteris P. 2008. Physiographically-sensitive mapping of temperature and precipitation across the conterminous United States. *International Journal of Climatology* **28**: 2031–2064.

Daly C, Helmer EH, Quinones M. 2003. Mapping the climate of Puerto Rico, Vieques, and Culebra. *International Journal of Climatology* **23**: 1359–1381.

Daly C, Smith JW, Smith JI, McKane R. 2007. High-resolution spatial modeling of daily weather elements for a catchment in the Oregon Cascade Mountains, United States. *Journal of Applied Meteorology and Climatology* **46**: 1565–1586.

Ekhart E. 1934. Neuere Untersuchungen zur Aerologie der Talwinde: die periodischen Tageswinde in einem Quertale der Alpen. *Beitrage zur Physik der Atmosphaere* **21**: 245–268.

Geiger R. 1966. *The Climate Near the Ground*. Harvard University Press: Cambridge, 611.pp.

Gustavsson T, Karlsson M, Bogren J, Lindqvist S. 1998. Development of temperature patterns during clear nights. *Journal of Applied Meteorology* **37**: 559–571.

Andrews HJ. 2007. *Experimental Forest*. Web site with meteorological data, http://www.fsl.orst.edu/lter/, Accessed on April 2008.

Intergovernmental Panel on Climate Change. 2007. Fourth Assessment Working Group I, *Climate Change 2007 – The Physical Science Basis, Chapter 11, Regional Climate Projections*, http://www.ipcc.ch/pdf/assessment-report/ar4/wg1/ar4-wg1-chapter11.pdf.

Kalnay E, *et al.* 1996. The NCEP/NCAR 40-year reanalysis project. *Beitrage zur Physik der Atmosphaere* **77**: 437–470.

Landsberg JJ, Waring RH. 1997. A generalised model of forest productivity using simplified concepts of radiation-use efficiency, carbon balance and partitioning. *Forest Ecology and Management* **95**: 209–228.

Lindkvist L, Gustavsson T, Bogren J. 2000. A frost assessment method for mountainous areas. *Agricultural and Forest Meteorology* **102**: 51–67.

Losleben M, Pepin N, Pedrick S. 2000. Relationships of precipitation chemistry, atmospheric circulation, and elevation, at two sites on the Colorado Front Range. *Atmospheric Environment* **34**: 1723–1737.

Lundquist JD, Cayan DR. 2007. Surface temperature patterns in complex terrain: daily variations and long-term changes in the central Sierra Nevada, California. *Journal of Geophysical Research* **112**: D11124. DOI: 10.1029/2006JD007561.

Lundquist JD, Pepin N, Rochford C. 2008. Automated algorithm for mapping regions of cold-air pooling in complex terrain. *Journal of Geophysical Research* **113**: D22107. DOI: 10.1029/2008JD009879.

Mahrt L, Vickers D, Nakamura R, Soler MR, Sun J, Burns S, Lenschow DH. 2001. Shallow drainage flows. *Boundary-Layer Meteorology* **101**: 243–260.

Marvin CF. 1914. Air drainage explained. *Monthly Weather Review* **10**: 583–585.

McChesney CJ, Koch JM, Bell DT. 1995. Jarrah forest restoration in Western Australia: canopy and topographic effects. *Restoration Ecology* **3**: 105–110.

McKee TB, O'Neal RO. 1989. The role of valley geometry and energy budget in the formation of nocturnal valley winds. *Journal of Applied Meteorology* **28**: 445–456.

Miller DR, Bergen JD, Neuroth G. 1983. Cold air drainage in a narrow forested valley. *Forest Science* **29**: 357–370.

Pearson RG. 2006. Climate change and the migration capacity of species. *Trends in Ecology and Evolution* **21**: 111–113.

Pepin N, Lundquist JD. 2008. Temperature trends at high elevations: patterns across the globe. *Geophysical Research Letters* **35**: L14701. DOI: 10.1029/2008GL034026.

Pepin N, Norris JR. 2005. An examination of the differences between surface and free-air temperature trends at high-elevation sites: Relationships with cloud cover, snow cover, and wind. *Journal of Geophysical Research* **110**: D24112. DOI: 10,1029/2005JD006150.

Poulos G, Zhong S. 2008. An observational history of small-scale katabatic winds in mid-latitudes. *Geography Compass* **2/6**: 1798–1821.

Pypker TG, Unsworth MH, Mix AC, Rugh W, Ocheltree T, Alstad K, Bond BJ. 2007. Using nocturnal cold air drainage flow to monitor ecosystem processes in complex terrain. *Ecological Applications* **17**: 702–714.

Rodrigo J. 2000. Spring frosts in deciduous fruit trees – morphological damage and flower hardiness. *Scientia Horticulturae* **85**: 155–173.

Tenow O, Nilssen A. 1990. Egg cold hardiness and topoclimatic limitations to outbreaks of Epirrita autumnata in northern Fennoscandia. *Journal of Applied Ecology* **27**: 723–734.

Whiteman, CD. 2000. *Mountain Meteorology: Fundamentals and Applications*. Oxford University Press: Oxford, 355pp.

Zangl G. 2005. Dynamical aspects of wintertime cold-air pools in an alpine valley system. *Monthly Weather Review* **133**: 2721–2740.